Positioning with Punctured GPS

Peter J. Duffett-Smith, University of Cambridge and Cambridge Silicon Radio
Anthony R. Pratt, Orbstar Consultants
Thomas Jost & Matthias Kranz, German Aerospace Center (DLR)

ABSTRACT

We examine reasons for interrupting the data stream from a GPS receiver integrated into a mobile phone, and the effects such interruptions have on the pseudorange and pseudorange rate determined by the receiver in tracking mode. We present measurements of the multi-path environment inside a small office at the Cavendish Laboratory, UK, and in the much-larger entrance hall of the German Space Operations Centre near Munich, Germany, and find that interruptions of several tens of seconds can be tolerated without serious impact on the positioning performance. This conclusion, if supported by measurements made in other environments typical of mobile-phone use, bodes well for the integration of GNSS receivers within mobile phones suitable for the mass market.

INTRODUCTION

GPS receivers incorporated into cellular telephones must necessarily work in close proximity with other electronic devices, posing challenges of interference and cooperative operation. The interference may be strong enough to disable the GPS receiver completely, for example during data bursts in a GSM transmission. In less extreme cases, it may cause the sensitivity of the GPS receiver to be degraded.

GPS signal reception can also be punctured in architectures employing common hardware resources for several functions, such as a shared antenna, a shared receiver chain, a shared digital signal processor or a shared I/O port. Clashes in demands for the use of these shared resources results from the need to minimise the hardware ‘real estate’ and/or processing load in order to reduce costs or power consumption. One example occurs in mobile cellular telephone applications where a common RF and IF processor for signal reception cannot generally be used for GPS and voice or data reception at the same time. In such cases, priority may be given to the voice or data connection, so that the GPS position-determining function is delayed until the resources are released. The duration of the delay may, or may not, be predictable. Even when all the other devices in the cellular telephone have been turned off, the useful GPS received signal samples may still be intermittent because of intensity fluctuations in environments where there is significant multi-path signal interference causing the signal-to-noise ratio to drop intermittently below a minimum sensitivity threshold.

Another limiting factor where a GPS (or other GNSS) receiver has been incorporated within a mobile device such as a mobile telephone, personal navigation device, or personal data aid, is the requirement to conserve battery energy in order to make the time between recharging as

long as possible. This implies that the GNSS receiver may not operate in continuous mode even when it is the only device running and has all the hardware and software resources of the portable device available to it. An exception to this is when such a device is mounted in a cradle or similar support attachment inside a vehicle. The device may then use the vehicle's power system (and also has the possibility of access to an external antenna) so that power availability during periods of operation is rarely limiting.

Most designers also rely on advances in technology to reduce power consumption, for example using integrated circuits with the smallest feature sizes. These advances have produced GPS designs with continuous power consumption well below 30 mW, but they require careful control of the signal processing architecture and digital processing clock frequencies, with inevitable trade-offs in GPS receiver performance.

In this paper, we explore the effects of such interruptions in the data stream on the pseudorange and pseudorange rate estimated by a GPS receiver. We consider an alternative methodology for power savings based on prediction of the pseudorange to each visible satellite at a future time based on the current measurements, enabling lock to be maintained when the receiver is switched off. How long this interval may be between GPS reception periods depends upon the reliability of the prediction, in turn dependent on knowledge of the error components measured along with the pseudorange. Error components include thermal noise, clock jitter, GPS time estimation error, error in the receiver's current position, and signal propagation effects such as multi-path. The most significant contribution may well be as a result of multi-path where significant signal obscuration occurs as in highly urban conditions or inside buildings.

PSEUDORANGE PREDICTION

Pseudorange can be predicted from a typical set of range measurements. An example of this is given in Figure 1. The graph traces out the range variations observed on SV13 in central Cambridge, UK. The shape of the curve can be modelled as a near parabola with some minor correction terms, determined using a non-linear regression. The coefficients of the third-order and subsequent power terms are much smaller than the second-order (parabolic) power term. The origin of the pseudorange model has been adjusted to eliminate the linear regression terms. For the specific measurements shown, taken on February 27th, 2008, the time of closest approach corresponded to 18 minutes and 14 seconds into the record. GPS time was determined from the data message and the receiver clock offset was corrected through a location solution. The origin of the left-hand vertical axis corresponds to 20,000 km, so it can be inferred that the satellite orbit passed close to the GPS receiver's zenith. Results were recorded every half second.

The blue curve in Figure 1 is a plot of the measured pseudorange and is to be read against the left-hand axis. The magenta curve represents the difference between the measurements and the model, is to a much smaller scale, and is to be read against the right-hand axis. The model retained power terms up to the third order, so that the pseudorange, ρ, was given by

$$\rho = a + bt^2 + ct^3,$$

with

$a = 20000$ km,

$b = 1.36 \times 10^{-5}$ m s^{-2},

$c = -1.7 \times 10^{-10}$ m s^{-3}.

The jagged characteristic was caused by quantisation of the receiver measurements. The error curve has peaks of less than 80 m. Exclusion of the 3rd order power terms significantly increases the peak error to about 2 km at the start and end of the interval for which the model is valid.

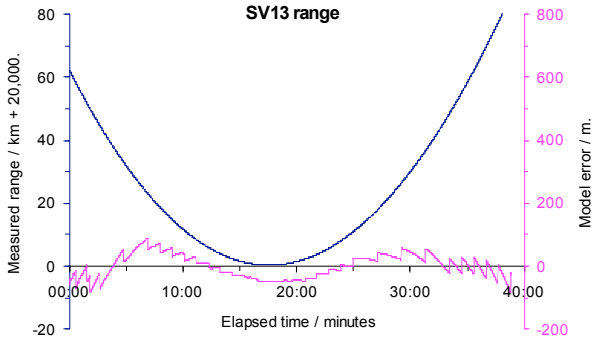

Figure 1: pseudorange measurements (dark-blue curve, left-hand scale) and prediction error (magenta curve, right-hand scale) using a low-order power-series model.

The conclusion to be drawn from this model is that ephemeris data for a specific satellite can be used to provide range predictions using an estimate of receiver location with a simple power series at accuracy levels appropriate to support re-acquisition i.e. better than one quarter of a chip (75 m). This conclusion has also been made by others [1], on the assumption that ephemeris and clock data are provided, but not in the context of punctured signal reception.

OPERATING MODES

The intervals during which operations of the GPS receiver are permitted or blocked depend upon external stimuli which the receiver is generally not able to control. These include the cellular wireless or Bluetooth transmission intervals, or signal loss caused by fading. The intent here is to probe how well, and for how long, previous measurements made by the GPS receiver, primarily of pseudorange and pseudorange rate (PR and PRR) can be relied upon to maintain the tracking window or assist the re-acquisition of GPS signals. Not surprisingly, the quality of the underlying signal model has a major impact on the interval for which the measurements can be used to provide an adequate (forward) prediction of the PR and PRR states.

There are various modes in which an embedded GPS receiver might operate. These include (a) outside, continuous; (b) outside, intermittent; (c) indoor, continuous; and (d) indoor, intermittent. The environmental characteristics are also significant. Of these, the most interesting one for analysis is case (d). In this case, the influence of multi-path errors and weak-signal conditions cause the signal reception to be interrupted by periods of C/N_0 below the threshold for signal acquisition or tracking, in addition to any enforced periods of non-availability. Furthermore, the prediction of future acquisition or tracking parameters (for example PR or PRR) is at its weakest as multi-path significantly disturbs the short-term estimates of these parameters.

INTERMITTENT OPERATION

For many embedded GPS receivers, the intermittent mode of operation has the most demanding characteristics. As already discussed, when indoors the signals may be punctured for two reasons, first because the GPS receiver loses access to critical resources, and second because the signal is too weak, either because of signal fading caused by obscuration (i.e. pure signal attenuation) or because of signal fading caused by multi-path interference (i.e. many signals of arbitrary phases in vectorial addition). The multi-path signal fading is usually observed in combination with signal attenuation. To model this effect, we assume that a GPS receiver is unable to maintain track or acquire signals below a specified threshold carrier to noise power ratio (C/N_0). Often the tracking failure occurs at lower C/N_0 than the acquisition failure because the tracking bandwidths are significantly narrower than those used for acquisition. A narrow tracking bandwidth requires a period maintained in tracking mode of at least several times the reciprocal of this bandwidth. Thus a 0.1 Hz tracking bandwidth implies a minimum time in track of 20-30 seconds. In many circumstances the dynamic properties of multi-path signals, especially when the GPS receiver is in motion, do not permit such durations in track, and much wider bandwidths must be used.

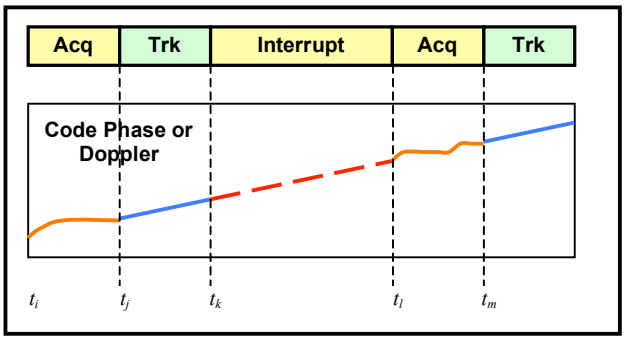

Figure 2: illustration of an acquisition and tracking Cycle

We show later in Figure 5 an example of a plot of the variation of C/N_0, recently obtained, for a static indoor antenna in a small office room with a single window. The antenna was located at a height similar to the middle of the window. For the purposes of this paper, we have assumed a threshold value of C/N_0 of 20 dB Hz, below which operation is not possible. For this level to represent a sensible threshold for tracking, it is only necessary to assume a modest non-

coherent integration time and 2 to 3 dB of receiver implementation losses, values easily justified with an integrated antenna with perhaps an efficiency of –3 dB, a modest receiver noise figure, and a two- or three-level ADC.

A normal operating mode for the GPS receiver, then, is one where interruption in signal reception is commonplace. In order to support this mode, the GPS receiver may expect to spend a disproportionate part of its operating time in acquisition rather than tracking mode. Providing the interruptions are not connected by long periods of non-operation, it may be possible to use the code phase and code phase rate and/or Doppler offset parameters from the previous tracking/acquisition event to aid the next signal acquisition. Figure 2 illustrates the propagation of previous acquisition/tracking parameters to future acquisition events.

As Figure 2 suggests, an acquisition period starts at time, t_i, and has an acquisition transient prior to commencing a tracking period during the time from t_j to t_k. After this time, the tracking is interrupted (because of one of the stimuli mentioned above, for example), before a further acquisition and tracking cycle recommence at t_l and t_m respectively. The illustrative curves could represent either the Doppler or code offset as a function of time.

At the end of a tracking event (e.g. at time t_k), the GPS receiver has determined estimates for the code phase and Doppler offsets and their rates of change, designated as follows:

ϕ_{t_k} is the code phase at t_k;

$\dot{\phi}_{t_k}$ is the code phase rate at t_k;

ω_{t_k} is the Doppler offset at t_k;

$\dot{\omega}_{t_k}$ is the Doppler offset rate at t_k.

In practice, the model for code phase and Doppler will not be able to be represented only by linear terms. Even if the underlying dynamic behaviour of the satellite and GPS host can be modelled in this way, the receiver clock and propagation conditions will still introduce a random component. Assuming for the moment that the random components can be represented by a correlated noise process, but with zero mean, then estimates of code phase and Doppler offset can be derived after a period of interruption as follows:

$$\hat{\phi}_{t_l} = \phi_{t_k} + \dot{\phi}_{t_k} \cdot (t_l - t_k),$$

$$\hat{\dot{\phi}}_{t_l} = \dot{\phi}_{t_k},$$

$$\hat{\omega}_{t_l} = \omega_{t_k} + \dot{\omega}_{t_k} \cdot (t_l - t_k),$$

$$\hat{\dot{\omega}}_{t_l} = \dot{\omega}_{t_k}.$$

The ‘hat’ over the symbols on the left-hand side of each equation represents the *a priori* estimate of the component at the start of the next acquisition cycle at t_l (before a new acquisition process has commenced). The actual value of any of the parameters can be represented in a Taylor’s series using all the differential terms:

$$\varphi_{T+t} = \varphi_T + \dot{\varphi}_T \cdot t + \ddot{\varphi}_T \cdot t^2 + \dddot{\varphi}_T \cdot t^3 + \ldots$$

where, for example,

$$\frac{\partial \varphi}{\partial t} = \dot{\varphi} \quad \text{and} \quad \frac{\partial^2 \varphi}{\partial t^2} = \ddot{\varphi} \quad \text{etc.}$$

The errors in the *a priori* estimates are contained in terms, ε_x, representing the error due to inadequate modelling (for example loss of all the Taylor series elements after the first differential) and the effects of random and propagation noise:

$$\hat{\phi}_{t_l} = \phi_{t_l} + \varepsilon_{PR},$$

$$\hat{\dot{\phi}}_{t_l} = \dot{\phi}_{t_l} + \varepsilon_{PRR},$$

$$\hat{\omega}_{t_l} = \omega_{t_l} + \varepsilon_{D},$$

$$\hat{\dot{\omega}}_{t_l} = \dot{\omega}_{t_l} + \varepsilon_{DR}.$$

For the linear model proposed, the best estimates for the code phase and Doppler rates are just the values for those parameters at the end of the previous tracking period. Typical receivers, using second-order tracking loops, have two receiver states represented in the loop. These are, for a code-tracking loop, the code phase (the output from the code NCO) and the code frequency (the input to the NCO). The filtered estimate of code frequency is held in an integrator in the loop filter. Similar states can be identified for a carrier frequency-tracking loop.

If a more complex model is considered, then code phase and Doppler acceleration parameters are also needed. Such parameters may be available in some receivers where tracking loops of third or higher order have been implemented. However, in many receivers, these higher-order loops also have the significant disadvantage that the acquisition transient is of longer duration than those in second-order loops. It has, therefore, been assumed that only second-order loops are, at best, implemented or, if a third-order loop has been used, that reception is terminated before it can reliably estimate the acceleration parameter value.

ASSISTED GPS

Many GPS receivers, used in conjunction with a cellular wireless host, will have GPS assistance available. This includes the provision of satellite almanac, ephemeris, satellite clock correction parameters, and estimates of location and approximate time. The ephemeris and approximate time can be used to form a pseudorange model for a specific receiver location. The model can then be used to remove the effect of satellite motion from the estimates of code phase. However, the benefits of this are not significant except for initial acquisition, or unless the period of interruption is long. If such a pseudorange model is used, only a few terms, as shown above, are required to provide satisfactory accuracy for several hours of satellite motion.

REACQUISITION AFTER INTERRUPTION

After a period of signal interruption, the GPS receiver will attempt to reacquire the signal using estimates of the code phase and Doppler frequency offset. If these are reliable representations of the actual parameter values at the time of reacquisition, then the reacquisition transient for the code and carrier tracking loops will be of short duration.

The question of how good are the *a priori* estimates can only be determined through practical measurements. The signal reception conditions and the period of interruption provide a matrix of qualifications to the estimation errors. One of the main objectives of the receiver design is to provide algorithms that minimise the re-acquisition transient. This ensures that the signal reception intervals are short. A second objective is to establish the duration of the tracking periods that will provide good estimates of the parameters for re-acquisition. These will depend upon the signal reception conditions – especially the value of C/N_0 and the stability of the code phase and Doppler offset in multi-path propagation environments.

In order to ensure a sensible pull-in (acquisition) transient for the code-tracking loop, the code error upon loop closure must be smaller than half a chip even under good C/N_0 conditions. As C/N_0 falls to lower values, the closed tracking loop becomes more sensitive to noise excitation and, consequently, the pull-in range shrinks. This can be further complicated in GPS receivers using a narrow RF bandwidth, as this also causes reductions in the usable range of the receiver's 'S' curve (its code detector characteristic). We have assumed, for the purposes of this paper, that a pull-in range of about $1/10^{th}$ of a chip can be reliably used.

In addition to reductions in the pull-in range, there is a minimum threshold value below which the signal cannot be detected reliably. In the experiments conducted here, the receivers have a lower operational threshold of C/N_0 = 20 dB Hz.

INDOOR MULTI-PATH: Measurements

We investigated the multi-path environments both inside a small office on the upper floor of a two-storey building at the Cavendish Laboratory in Cambridge, UK (Figure 3a), and in the spacious entrance hall of the German Space Operations Centre near Munich (Figure 3b), by measuring its effect on the estimated pseudorange. The Cavendish Laboratory building was of block construction within a steel frame and a flat roof. Direct line-of-sight signals from the sky, though attenuated, were probably picked up by the antennas. The GSOC building, on the other hand, was a substantial steel and concrete construction of several stories. The direct line-of-sight signals were almost certainly attenuated sufficiently to render them much smaller than signals reflected from external buildings. We used a CSR-Nordnav GPS multi-receiver [4] (see Figure 4) which comprised three independent hardware front-ends and digitisers, and a separate software processor. This flexible design allowed for one of the receivers, labelled 1 in Figure 4, to be designated as the master receiver, and two others, labelled 2 and 3, to be designated as slaves. The master receiver was connected to an active patch antenna placed on the roof of the building with a clear view of the sky. The master receiver was set to track six satellites and establish a position and time solution. Each of the slave receivers was connected

to an active patch antenna. The lower panel in Figure 3a (small office) shows the antennas placed on top of a metal filing cabinet at the back of the room, well away from the window. The lower panel in Figure 3b (large entrance hall) shows the antennas placed on the floor. Although the antennas incorporated low-noise preamplifiers with about 28 dB of gain, it was nevertheless found to be beneficial to include additional amplifiers, providing good isolation and a further 20 dB of gain, as shown in Figure 4.

(a) (b)

Figure 3: views of (a) outside the two-storey building (upper panel) and inside the small office (lower panel), and (b) inside the entrance hall of GSOC (upper panel) and the antenna arrangement (lower panel).

The tracking parameters measured by the master receiver for two of the satellites were used to constrain the tracking windows for those satellites in the slave receivers 2 and 3, with the result that the indoor tracking sensitivity was enhanced by more than 20 dB. This enabled the two indoor receivers to make meaningful estimates in the indoor environment both of the carrier-to-noise ratio, C/N_0, and the pseudorange offset, $|\Delta \boldsymbol{r}|$. The latter was defined as follows: if $\boldsymbol{r}_1$ was the vector position of an SV relative to antenna 1, and $\boldsymbol{r}_3$ the vector position of the SV from antenna 3 (see Figure 4), then the (pseudo) range offset was defined as

$$|\Delta \boldsymbol{r}_3| = \boldsymbol{r}_1 - \boldsymbol{r}_3,$$

and similarly for $|\Delta \boldsymbol{r}_2|$. We found that the indoor measurements of $|\Delta \boldsymbol{r}|$ were repeatable for C/N_0 values greater than 20 dB Hz. Typical examples of measurements taken in the small office are shown in Figures 5 and 6.

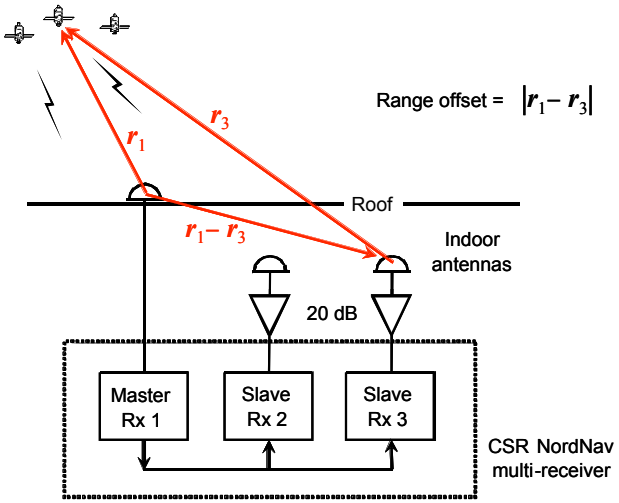

Figure 4: the measurement system

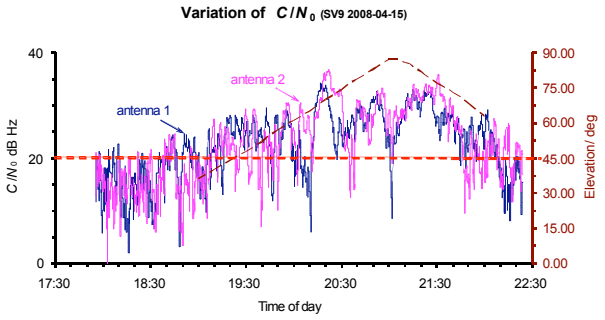

Figure 5: the variation of C/N_0 measured by the indoor receivers for SV9 on 15th April, 2008. in the small office.

Figure 5 shows the variation in C/N_0 (left-hand scale) measured by indoor receivers 2 (dark blue) and 3 (magenta) on 15th April, 2008 for SV9 in the small office. In this case, the indoor antennas were spaced 5 cm apart along the EW line. Only data above the horizontal dashed red line denoting 20 dB Hz are trustworthy and have been used in the analysis. Also shown is the elevation of SV9 (right-hand scale), and it is not surprising to see that the temporal variations were slowest, and the C/N_0 values generally highest, when the satellite was at high elevations.

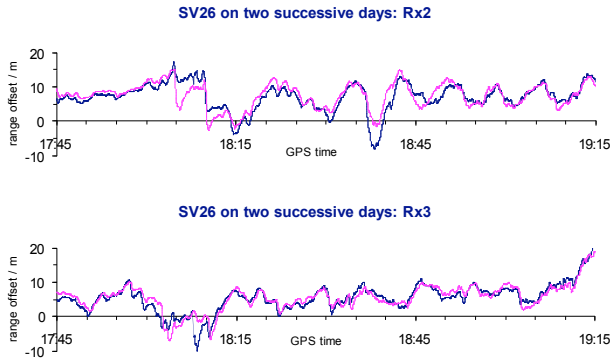

Figure 6: plots of the range offset measured for SV26 by receiver 2 (upper panel) and receiver 3 (lower panel) on the 12th (dark blue) and 13th (magenta) April, 2008, in the small office. The values for the 13th have been shifted earlier by about 4 min.

Figure 6 demonstrates that the measurements were repeatable. Here, measurements of the range offset, $|\Delta \boldsymbol{r}|$, taken on two successive days, are plotted against time of day for SV26. The antenna positions were unchanged on the two days, but the data for the second day have been shifted early by about 4 minutes before plotting. The track of the satellite in the sky was expected to be similar on two successive days except for a time shift corresponding to the difference of about 4 minutes between the sidereal day and the solar day. The fact that the variations seen by the two receivers closely match each other after this shift has been taken into account provides strong evidence that they were caused by multi-path effects, and gave us confidence that the data corresponding to values of C/N_0 greater than 20 dB Hz were meaningful.

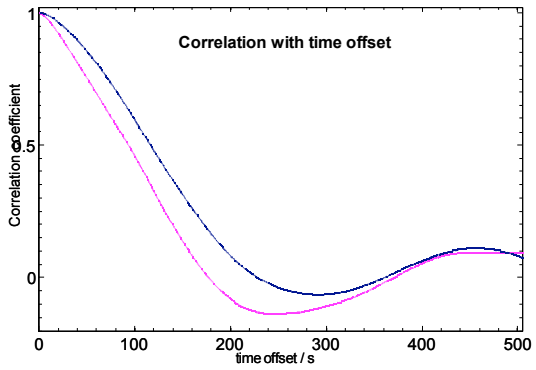

Figure 7: the temporal correlation coefficient plotted against time offset for the data shown in Figure 6.

The tracking points in both the master and slave receivers were determined by fitting a curve to the top three points of the cross-correlation. The measurements of pseudorange offset therefore demonstrate the effect of the distortion introduced by the multi-path environment on the shape of the peak of the cross-correlation function.

The measurements taken on a single day in both environments typically show slow quasi-sinusoidal variations on a time scale of about 100 s, and of amplitude about 10 m (small office) or perhaps several tens of metres (large entrance hall). The temporal correlation is illustrated in Figure 7 where the autocorrelations of the data shown in Figure 6 for 12th April, 2008 are plotted against time offset (receiver 2 in blue and receiver 3 in magenta). The autocorrelations are similar for the two receivers, even though the plots in Figure 6 are quite different from each other, and they suggest that the affects of the multi-path on the pseudorange are predictable for more than 100 s into the future (in the static channel case).

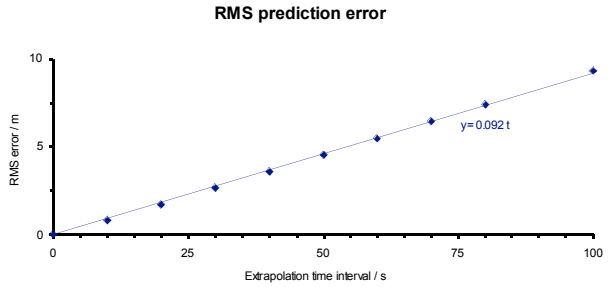

Figure 8: the difference between predicted and measured pseudorange as a function of extrapolation interval.

This is further demonstrated in Figure 8 where the predicted pseudorange offset, estimated from an extrapolation of a straight-line fit to five-seconds worth of measurements, is compared with the measured values. Figure 8 was derived from the measurements as follows. We denote the i^{th} data value in a time series of consecutive measurements of the pseudorange offset by d_i. The set of N consecutive values, beginning at the point $i = j$, are used as the basis for the extrapolation. In this case, N = 10 since the data were taken every half second. A linear regression was performed on the N values $\{d_j, d_{j+1}, d_{j+2}, \ldots, d_{j+N-1}\}$ to find the slope, m, and the intercept, c, using least-squares fitting. The extrapolation over an interval of T seconds, corresponding to $M = 2T$ values, produced the estimated data value D_M given by

$$D_M = m(j+N-1+M) + c \ .$$

The rms of the difference between the estimated and measured values, i.e. $d_{j+N-1+M} - D_M$, was found over all possible points from the start to the end of the record, about 14,000 points. The analysis was repeated for value of T = 10, 20, 30 .. etc. s, and the resulting rms values were plotted on the graph.

INDOOR MULTI-PATH: Spatial correlation

The spatial correlation of the multi-path environment was also investigated by making measurements at various different separations of the indoor antennas. In the small office, the range from 5 to 20 cm was investigated, roughly from a quarter of a wavelength to one wavelength. In the large entrance hall, the range extended to about 15 wavelengths. Figure 9 shows a typical plot of the pseudorange offset measured as a function of time of day by

receivers two and three inside the small office. In this case, the antennas were only 5 cm apart along an East-West line, barely a quarter of a wavelength, yet the plots are quite different from each other. This is expected for strong multi-path interference from many scattering centres and is indicative of a Rayleigh channel.

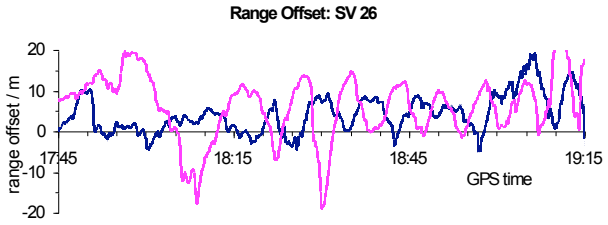

Figure 9: the pseudorange offset measured with receivers 2 (dark blue) and 3 (magenta) for SV26 on 15th April, 2008, in the small office. The antennas were 5 cm apart along an EW line.

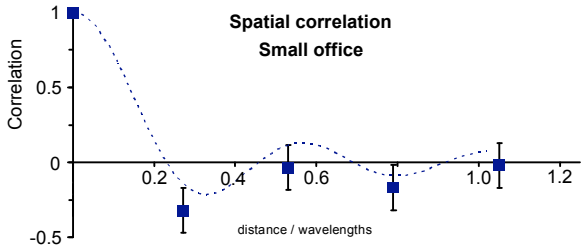

Figure 10: the spatial correlation coefficient of the indoor multi-path environment as a function of the distance between the antennas in the small office. (The dotted curve is suggestive, and serves only to guide the eye.)

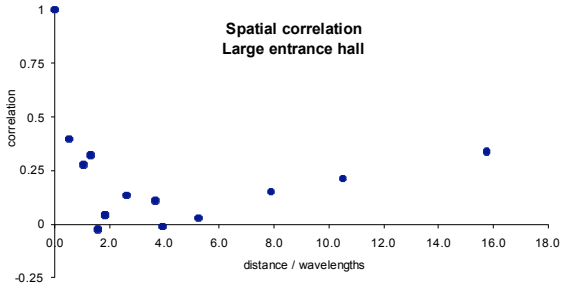

Figure 11: the spatial correlation coefficient of the indoor multi-path environment as a function of the distance between the antennas in the large entrance hall.

The measured spatial correlation functions are shown in Figures 10 and 11. Each point represents the normalized zero-lag cross-correlation coefficient between plots such as those of Figure 8, after removal of a mean offset from each plot. The offset was expected from the fact that the electrical paths from the satellites to the receivers were different for the antenna on the roof and the indoor antennas.

It is clear from the figures that the correlation drops rapidly within the first quarter of a wavelength separation in both environments, indicating that even a small movement of the antenna would have a large effect on the vectorial mix of multi-path signals received by it. However, there remains substantial cross-correlation power in the large entrance hall for separations of several tens of wavelengths. This surprising result supports the work reported by Jost and Robertson [3] in which measurements were made in the same environment using an array of small independent receivers (Figure 12). The good agreement between the two sets of results indicates that the same multi-path effects were being measured in each case, although there appears to be a systematic difference between them which needs further investigation.

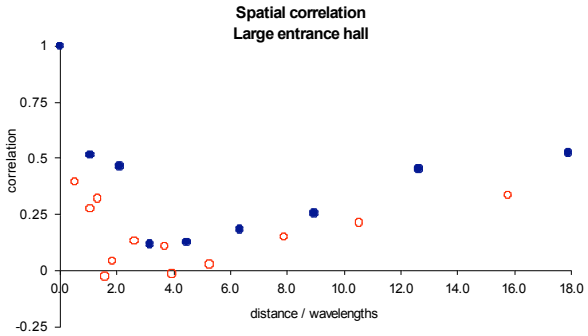

Figure 12: measurements of the spatial correlation function reported by Jost and Robertson [3] (filled blue circles) and in this paper (open red circles).

INDOOR MULTI-PATH: Analysis

The results shown in the previous sections indicate that the multi-path encountered inside the particular environments which were tested had the following broad characteristics:

1. The carrier-to-noise ratio, C/N_0, was sufficiently large (i.e. greater than 20 dB Hz) to give useful results when the satellites were above about 45 degrees elevation (small office).
2. Measurements of the pseudorange difference may have been in error by up to about ±10 m because of the multi-path (small office) or by several tens of metres (large entrance hall).
3. Measurements of the pseudorange difference made with static antennas exhibited slow quasi-sinusoidal variations with periods of tens of seconds, caused primarily by the satellite motion inducing slow changes to the (many) signal propagation paths.
4. The correlation of the measurements of the pseudorange difference with time extended over many tens of seconds.
5. The spatial correlation of measurements of the pseudorange difference fell rapidly with antenna separation and was near zero beyond a few cm, although it rose again for separations beyond 1 m in the case of the large entrance hall. (These separations were not investigated in the small office.)

Item 1 suggests that, for a GNSS receiver incorporated into a mobile terminal used indoors, it may generally be a waste of time and terminal resources to attempt to make any measurements at all on satellites which are low in the sky, only those above an elevation of, say, 50 degrees being potentially useful. If there are no such satellites available, the terminal would need to fall back on an alternative positioning method, such as the Matrix method [2]. Items 2-5 suggest that multi-path may not be much of an issue in some indoor environments (such as those tested here). The maximum tracking error from multi-path encountered when extrapolating across a gap of many tens of seconds was likely to be less only a few tens of metres, whether the terminal was moving or not, and this could have easily been accommodated within the tracking loop without reacquisition. This hypothesis, based on the measurements made in the two environments described here, would need testing in many more representative indoor places. Where multi-path errors have much larger amplitudes, items 2-4 suggest that, for a static channel, the effect of the multi-path on the measured pseudorange can be predicted over intervals of tens of seconds.

Turning now to item 5, the spatial correlation functions shows that when the terminal is moving, even at a walking pace, for example at 2 m s^{-1}, the effect on the multi-path component of the measured pseudorange decorrelates within 20 ms. The rate of decorrelation with time is dependent on the speed, with more rapid decorrelation at higher speeds. It is possible to propose a power spectral density function for the multi-path induced pseudorange noise. This could be computed (if we had an mathematical representation of the spatial correlation function) using standard Wiener-Kinchine techniques. In all likelihood, the result would show the characteristics of a low pass spectrum, i.e. flat at low frequencies with a characteristic cut-off based on the frequency at which quarter-wavelength transitions are made at the specific host velocity. Consequently, the upper frequency limit will be in the region of 20υ Hz where the speed is υ m s^{-1}.

The estimation error in the post-interruption code phase from pseudorange multi-path effects does not appear to amount to more than a few tens of metres (in the case of the environments studied here). It is likely that a moving receiver is more sensitive to the effects of errors in the pseudorange rate as estimated after a short period of tracking. This is barely sufficient for any signal acquisition process and inadequate for transition to a tracking mode.

The pseudo-range rate (PRR) may be obtained in simple tracking systems by differentiating the pseudorange measurements. This will induce a power spectral density with a rising frequency characteristic (as ω^2). We have not yet conducted tests to establish the correctness of the assumptions and results. However, an illustrative power spectral density function for the pseudorange (red curve) and pseudorange rate (blue curve) is provided in Figure 13. It is clear that filtering of the pseudorange rate would rapidly reduce the standard deviation of the estimate because the power spectral density falls quickly as the frequency range is reduced. The only residual issue then is the latency of the pseudorange rate estimate – as this grows the estimation accuracy would also fall.

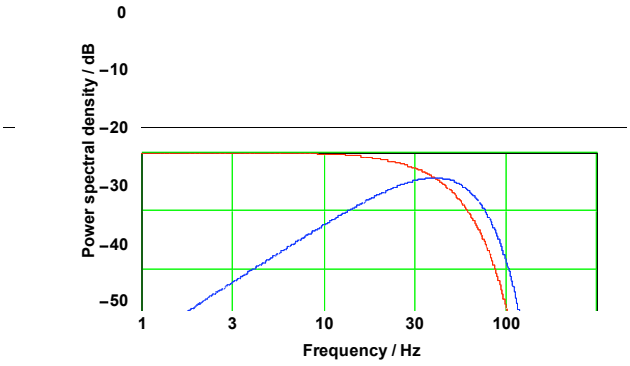

Figure 11: illustrative power spectral density curves for pseudorange (red) and pseudorange rate (blue).

CONCLUSIONS

We find that the effects of puncturing the data stream on the estimation of the pseudorange and pseudorange rate by a GPS receiver in tracking mode in two indoor environments would not be severe enough to limit its positioning performance. The multi-path errors were well within ± one tenth of a chip in pseudorange, so that the re-acquisition transient after a period of dormancy was likely to be small enough to be acceptable. The effect on the pseudorange rate, however, was highly sensitive to the speed of the receiver. At a speed appropriate to a fast walking pace, the power spectral density would rise steadily with frequency and turn over at about 50 Hz, suggesting that averaging for a period of, say one tenth of a second would yield a good estimate of the rate. Testing in many environments typical of mobile-phone use is needed to test these conclusions.

ACKNOWLEDGMENTS

The authors gratefully acknowledge the support of Sasha Mitelman in setting up the multi-channel GPS receiver, and of DLR for supporting the work measurement campaign in the large entrance hall.

REFERENCES

1. *Acquisition of GPS Signals at Very Low Signal to Noise Ratio*, Chansarkar M., & Garin, L., Proceedings of ION NTM 2000, 26-28 January 2000, Anaheim.

2. *Matrix, and Enhanced Satellite Positioning*, Duffett-Smith, P. J. & Craig, J., Proceedings of the IEE meeting 3G 2004, November 2004.

3. *Statistical Characterisation of the Indoor Pseudorange Error using Low Cost Receivers*, Jost, T. & Robertson, P., Proceedings of ION PLANS 2008, May 2008, Monterey.

4. *The Nordnav Indoor GNSS Reference Receiver*, Mitelman A., Normark P-L, Reidevall M., Thor J., Grönqvist O. & Magnusson L. Proceedings of ION GNSS meeting, September 2006, Fort Worth.